# Platform Precision Autopilot Overview and Flight Test Results

V. Lin[1], B. Strovers[2], J. Lee[3], and R. Beck[4]
*NASA Dryden Flight Research Center, Edwards, CA, 93523*

**The Platform Precision Autopilot is an instrument landing system–interfaced autopilot system, developed to enable an aircraft to repeatedly fly nearly the same trajectory hours, days, or weeks later. The Platform Precision Autopilot uses a novel design to interface with a NASA Gulfstream III jet by imitating the output of an instrument landing system approach. This technique minimizes, as much as possible, modifications to the baseline Gulfstream III jet and retains the safety features of the aircraft autopilot. The Platform Precision Autopilot requirement is to fly within a 5-m (16.4-ft) radius tube for distances to 200 km (108 nmi) in the presence of light turbulence for at least 90 percent of the time. This capability allows precise repeat-pass interferometry for the Uninhabited Aerial Vehicle Synthetic Aperture Radar program, whose primary objective is to develop a miniaturized, polarimetric, L-band synthetic aperture radar. Precise navigation is achieved using an accurate differential global positioning system developed by the Jet Propulsion Laboratory. Flight-testing has demonstrated the ability of the Platform Precision Autopilot to control the aircraft within the specified tolerance greater than 90 percent of the time in the presence of aircraft system noise and nonlinearities, constant pilot throttle adjustments, and light turbulence.**

## Nomenclature

| | | |
|---|---|---|
| Abs | = | absolute value |
| AIC | = | autopilot interface computer |
| CAN | = | controller area network |
| CPU | = | central processing unit |
| DAC | = | digital-to-analog converter |
| DCAPS | = | data collection and processing system |
| deg | = | degree |
| DFRC | = | Dryden Flight Research Center |
| dGPS | = | differential global positioning system |
| ECEF | = | Earth centered, Earth fixed |
| G-III | = | Gulfstream III jet |
| GPS | = | global positioning system |
| HIL | = | hardware-in-the-loop |
| I2S | = | ILS interface system |
| ILS | = | instrument landing system |
| INS | = | inertial navigation system |
| JPL | = | Jet Propulsion Laboratory |
| *K* | = | discrete time step |
| KIAS | = | knots indicated airspeed |
| MSR | = | maximum specific range |
| *P* | = | roll rate, deg/s |
| PPA | = | Platform Precision Autopilot |

[1] Aerospace Engineer, Flight Controls and Dynamics Branch, P.O. Box 273, M/S 4840D.
[2] Aerospace Engineer, Flight Controls and Dynamics Branch, P.O. Box 273, M/S 4840D.
[3] Aerospace Engineer, Flight Controls and Dynamics Branch, P.O. Box 273, M/S 4840D, AIAA Senior Member.
[4] Aerospace Engineer, Analytical Mechanics Associates, Inc, 4910 University Square, Ste 2, Huntsville, AL 35816.

| | | |
|---|---|---|
| $Q$ | = | pitch rate, deg/s |
| $R$ | = | yaw rate, deg/s |
| RF | = | radio frequency |
| RPI | = | repeat-pass interferometry |
| SAR | = | synthetic aperture radar |
| UAVSAR | = | Uninhabited Aerial Vehicle Synthetic Aperture Radar |
| $X$ | = | ECEF $X$-axis, m |
| $Y$ | = | ECEF $Y$-axis, m |
| $Z$ | = | ECEF $Z$-axis, m |
| $\Delta\Psi$ | = | change in heading angle, deg |
| $\Theta$ | = | pitch angle, deg |
| $\Lambda$ | = | nine element final observation vector, containing dGPS and INS terms |
| $\Phi$ | = | roll angle, deg |

## I. Introduction

Within the Earth science community, there is a growing need and desire for accurate Earth deformation measurements, which assist in the study and understanding of dynamically changing geological features resulting from earthquakes, volcanoes, and ice cap changes.[1,2] A synthetic aperture radar (SAR) provides this capability through a combination of active remote sensing, high-resolution mapping, and repeat passes over the area of interest. The SAR systems use a moving platform to create a narrow effective beam of electromagnetic waves and complex postprocessing to generate a detailed image. The phase data from two observation passes of the same terrain are compared by applying a technique known as interferometric SAR; any phase difference indicates terrain movement.[3,4]

Because of the time varying nature of rapidly deforming features, scientists require observational sampling intervals of a day or less to capture and model these events.[5] Most SAR systems are currently implemented on satellites, which have much longer repeat orbit cycles, on the order of weeks or even months. This aspect limits the effectiveness of these assets in the study of quickly deforming features. In its latest configuration, the NASA Airborne Synthetic Aperture Radar (AIRSAR)[6,7] system was able to demonstrate quick repeat observations when integrated on the NASA DC-8 (McDonnell Douglas, now The Boeing Company, Chicago, Illinois) Airborne Laboratory. The AIRSAR lacked track repeatability, however, which is an important factor for interferometry to work correctly. The resolution and accuracy of the DC-8 navigation architecture were insufficient to perform precision trajectory and repeat-pass interferometry (RPI). When implemented on any airborne platform, RPI is difficult for three main reasons:

1) Turbulence, wind gusts, and other varying atmospheric conditions make it difficult to fly the same path at different times.
2) A high precision navigation capability is required.
3) Varying crosswinds makes it difficult to maintain the same antenna pointing on repeated passes.[8]

In the 1990s, the Danish Center for Remote Sensing (DCRS, Lyngby, Denmark) conducted a project to attempt to resolve these complications with airborne RPI. Using a Danish Air Force Gulfstream III jet (G-III, Gulfstream Aerospace Corporation, A General Dynamics Company, Savannah, Georgia), the DCRS was able to demonstrate precision autopilot operation.[9] Modeled after this DCRS project, the NASA Uninhabited Aerial Vehicle Synthetic Aperture Radar (UAVSAR) program, the successor to AIRSAR, has used similar methods to overcome these challenges as well. The UAVSAR system has the capability to conduct radar RPI measurements with observational sampling intervals ranging from minutes to years, allowing surface measurements of centimeter level accuracy.

The UAVSAR program is supported by the NASA Dryden Flight Research Center (DFRC, Edwards, California) and led by the Jet Propulsion Laboratory (JPL, Pasadena, California). The primary objective of the UAVSAR program is to develop a miniaturized, polarimetric, L-band SAR for use on an uninhabited aerial vehicle (UAV) or minimally piloted vehicle. A G-III, as shown in Fig. 1, was selected as a demonstrator aircraft because of several performance criteria, including a range of greater than 3,000 nmi (5556 km), maximum altitude of 45,000 ft (13.72 km), adequate payload capability, and the ability to carry researchers during developmental test phases. The eventual goal of the project is to transition the SAR pod onto a UAV platform.


**Figure 1. NASA Gulfstream III jet carrying miniaturized polarimetric L-band synthetic aperture radar.**

The DFRC played a crucial role in the project as the developer of the Platform Precision Autopilot (PPA), an enabling technology that allows the UAVSAR to perform precise repeat-pass interferometry. This report describes the design, analysis, and flight test results of the PPA.

## II. Platform Precision Autopilot

An essential element for the success of the UAVSAR program is the PPA. The PPA interfaces with the G-III by imitating the output of instrument landing system (ILS) antennas. This technique has several advantages; system modifications to the baseline G-III are minimized by interfacing with the aircraft's ILS system, and some of the built-in safety features of the G-III systems and autopilot are retained. Examples of the applicable safety features are the aircraft autopilot rate and saturation limits on the localizer (lateral guidance) and glide slope (vertical guidance) to prevent any excessive maneuvers.

The PPA generates commands that drive two ILS interface system (I2S) units, which are two modified ILS testers, to produce modulated radio frequency (RF) signals. These RF signals are fed to the aircraft navigation receiver, which then directs the G-III autopilot to fly a constant-altitude ILS approach to meet the PPA requirements for the UAVSAR. The primary PPA objective is to make repeat-pass flights within a 5-m (16.4-ft) radius tube over a 200-km (108-nmi) course in conditions of calm to light turbulence[10] for 90 percent of the time. In addition, for the best performance of JPL's L-band SAR, operating on a steady platform is important. Hence, as a secondary objective, the PPA has to minimize motion of the G-III during data collection runs. The goals for pitch, roll, and yaw angle, and rate variation are as follows:

- Maintain roll angle variation within 5 deg peak to peak and roll rate within 0.45 deg/s.
- Maintain pitch angle variation within 5 deg peak to peak and pitch rate within 0.45 deg/s.
- Maintain yaw angle variation within 15 deg peak to peak and yaw rate within 1 deg/s.

Note that JPL requires the aircraft to maintain a nearly constant ground speed for the SAR. Without an auto-throttle capability on the G-III, the pilots must continuously manipulate the throttles to maintain a constant ground speed. Moreover, the G-III throttles are not instrumented; therefore, the PPA can respond only to resulting altitude changes caused by throttle manipulation.

## III. Hardware

The PPA is composed of three major hardware elements: the autopilot interface computer (AIC), I2S, and the PPA operator station. Figure 2 shows the PPA system architecture and the interfaces between these major hardware components and the G-III aircraft systems, which include the navigation receiver, flight director, and baseline autopilot. The AIC and I2S units, along with a power distribution panel, are designed to fit on a single pallet, which interfaces to the standard G-III cabin experimenter's rack (Fig. 3). With the addition of JPL's differential global

positioning system (dGPS) and a data acquisition research instrumentation system called the data collection and processing system (DCAPS), the PPA has all the necessary hardware to command the G-III autopilot.

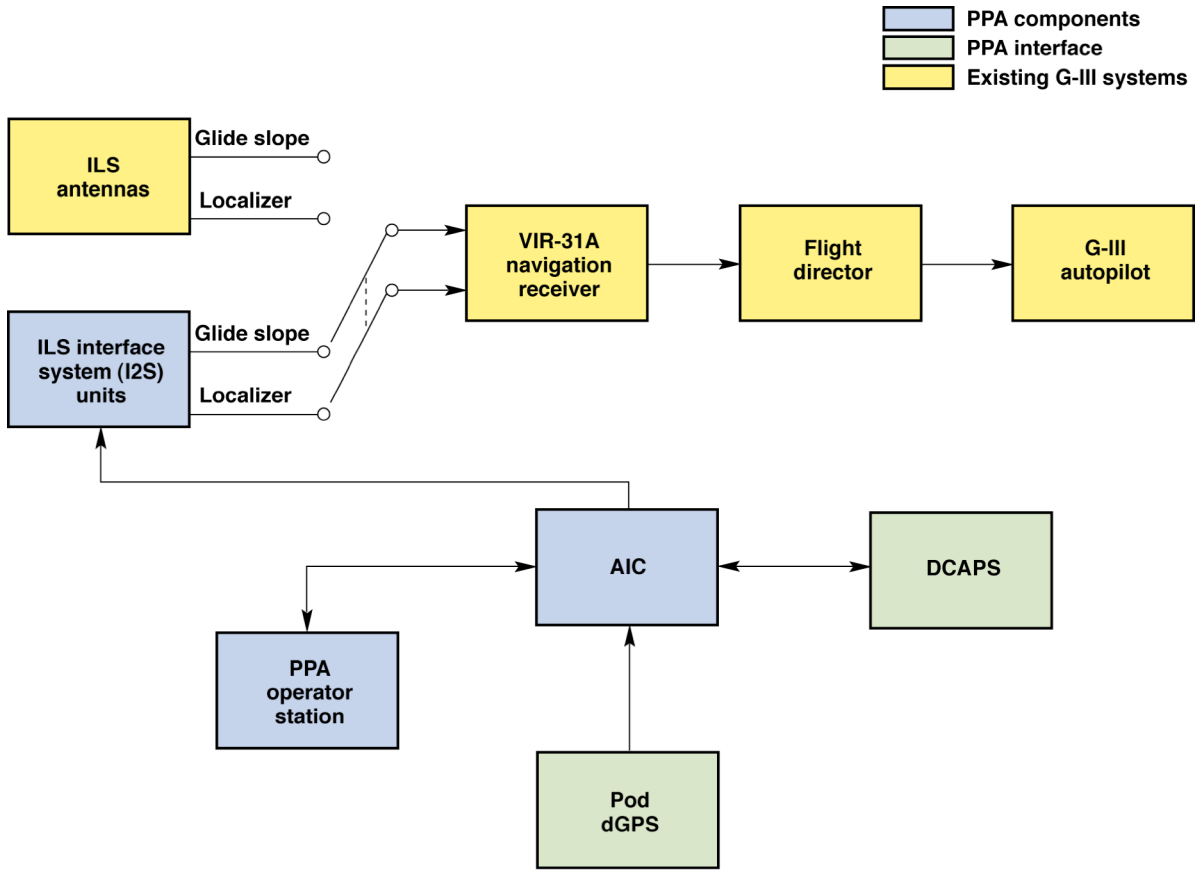


**Figure 2. Platform Precision Autopilot system architecture.**

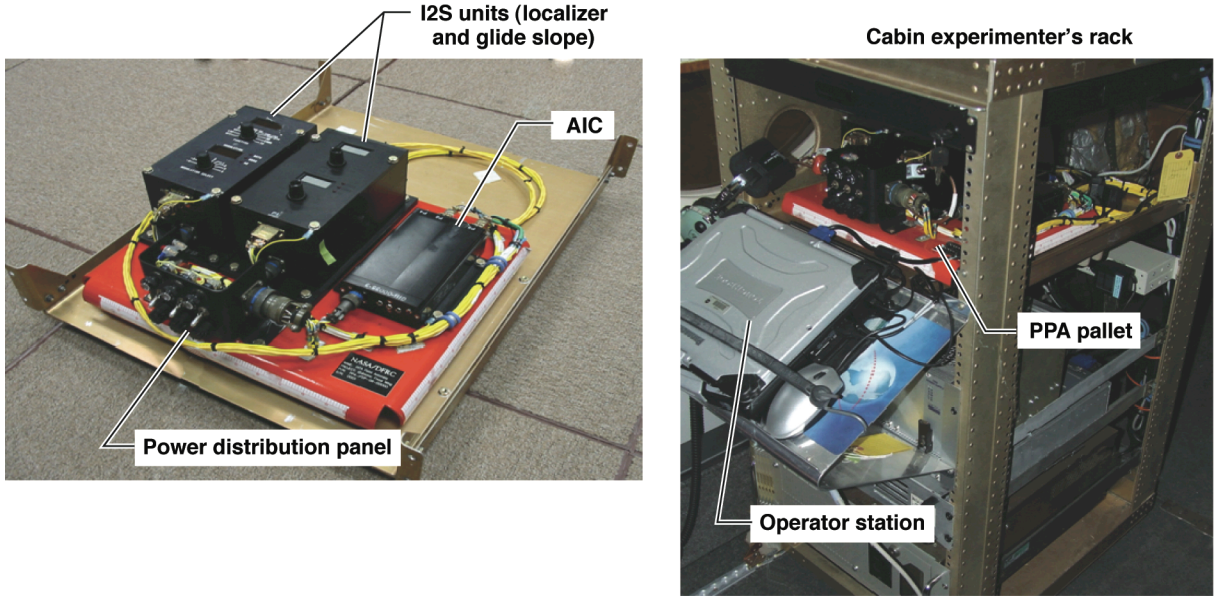


**Figure 3. Platform Precision Autopilot pallet and cabin experimenter's rack.**

### A. Autopilot Interface Computer

The AIC hosts the PPA software routines, which consist of *C* auto-code. This miniature computer is housed in a 6- by 3.5- by 1.625-in. enclosure and has a total weight of no more than 1.66 lb. The processor consists of a Phytec MPC565-based microcontroller (Phytec America, LLC, Bainbridge Island, Washington) mounted on a single board computer module operating at 56 MHz. Also included in the AIC are all the necessary power and signal conditioning elements. Figure 4 shows the PPA software architecture and external interfaces. The AIC provides a controller area network (CAN) interface with the operator station, RS-422 interface with the dGPS, and EtherNet® (Xerox Corporation, Palo Alto, California) interface with the DCAPS. Additionally, the AIC generates analog commands using a digital-to-analog converter interface and transmits them to the two I2S units.

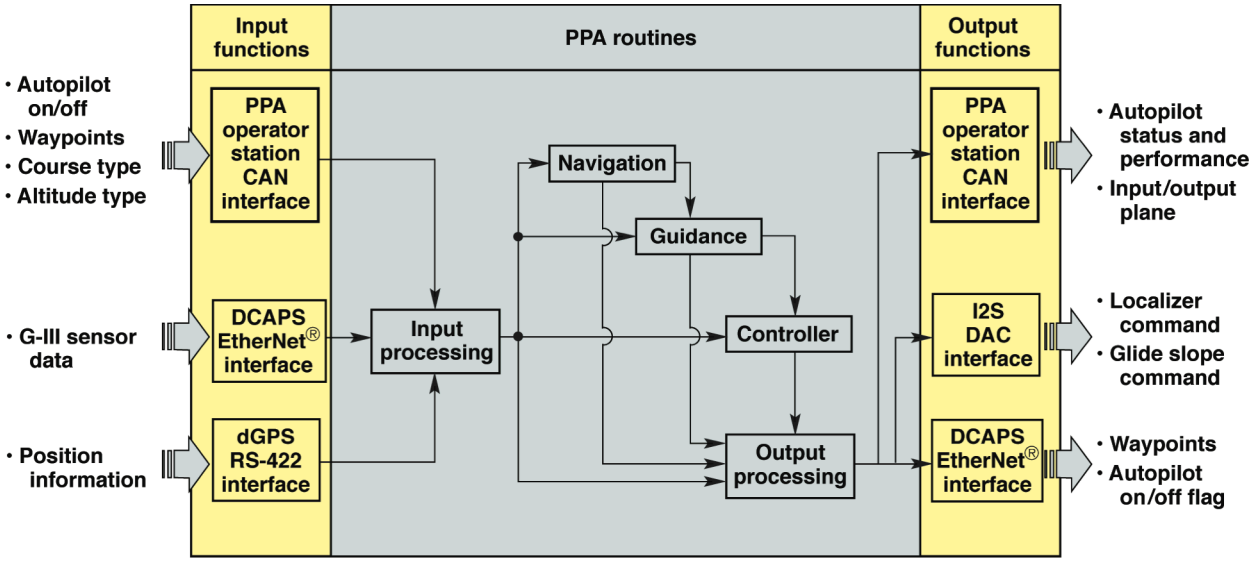


**Figure 4. Platform Precision Autopilot software architecture and external interfaces.**

### B. Instrument Landing System Interface

An I2S unit consists of a modified ILS ramp tester, which is capable of generating localizer or glide slope RF test signals needed to drive the G-III navigation receiver. The two I2S units receive analog voltage commands from the AIC. To independently modulate glide slope and localizer signals, two units are required. One I2S is commanded with a glide slope input and set for glide slope RF output, and the other is commanded with a localizer input and set for localizer RF output.

The analog voltage commands are sent to the two I2S units from the AIC through separate output channels with a resolution of 12 b, and a range of ±1.024 V. Using these commands, each I2S transmits one RF signal modulated at 90 and 150 Hz. The modulated RF signals are then routed to the aircraft navigation receiver through pilot-controlled RF switches. These switches give the pilots authority to select either the PPA or G-III navigation receiver antennas. The navigation receiver on the G-III then measures the difference in depth modulation (DDM) of the two ILS tones. The DDM between the two signals varies based on the deviation of the aircraft from the specified trajectory. Consequently, the I2S units generate the proper DDM of the ILS tones based on glide slope and localizer analog input levels.

### C. Operator Station

The operator station, which runs LabWindows™/CVI (C-Language Virtual Instrument, National Instruments Corporation, Austin, Texas), is the graphical user interface to the PPA. Using a CAN data bus, the operator station communicates with the AIC to monitor its status and serve the following functions:

1) Selects altitude and course path type
2) Initializes navigation software routine
3) Allows zeroing of biases
4) Initiates built-in tests
5) Engages and disengages PPA
6) Uploads waypoint file for trajectory generation

7) Displays and records data for postflight analysis
8) Displays status information, including data validity.

### D. Data Collection and Processing System

The DCAPS is the principle instrumentation system on the G-III. Developed at DFRC, DCAPS is largely a passive system that collects and archives aircraft state and instrumentation data through the G-III ARINC-429 bus, and distributes and displays it real time.[11] Using a 40-Hz user data protocol (UDP) link through the EtherNet® interface operating at 10 Mb/s, the DCAPS provides navigation data to the AIC.

### E. Differential Global Positioning System

The dGPS unit, designed by JPL, provides Earth centered, Earth fixed (ECEF) position in meters. It achieves high accuracy by using two sources of GPS correction communicated through Inmarsat (Inmarsat, plc, London, England) and Iridium (Iridium Satellite, LLC, Bethesda, Maryland) satellite systems, and two differential GPS units. Four position solutions are computed, and the best solution is automatically selected and output at 1 Hz. The dGPS 1-$\sigma$ position accuracy is estimated at 10 cm horizontally and 20 cm vertically.

## IV. Software

The PPA software runs at 40 Hz and is composed of MATLAB® functions and Simulink® block diagrams auto-coded into *C* code using the Real-Time Workshop® embedded coder (MATLAB®, Simulink®, and Real-Time Workshop® are registered trademarks of The MathWorks™, Inc., Natick, Massachusetts). The architecture of the software (Fig. 4) is broken down into three main subsystems: navigation, guidance, and controller. With the addition of input processing and output processing, which are two minor subsystems that perform signal routing, the three main subsystems are able to achieve the requirements set forth for the PPA.

### A. Input and Output Processing

The input and output processing routines provide data routing functionality. Input processing arranges and sends certain signals to the navigation, guidance, and controller routines. Input processing also performs invalid data detection for out-of-limit or stale values. For certain signals, such as dGPS *X*, *Y*, and *Z* positions, if values are saturated for one sample, the signals are declared failed. If signals are stale for more than 5 s, they are declared failed. Either failure will send a flag to the operator station indicating the presence of bad data. The output processing routine packages signals from the three main subsystems for routing to the operator station, I2S, and DCAPS.

### B. Navigation Routine

The navigation routine centers around a MATLAB® *m*-file designed to be called as an embedded function in Simulink®. The navigation filter (Fig. 5) generates an accurate position estimate using 1-Hz lagged position measurements from the dGPS and 16-Hz velocity data from the aircraft inertial navigation system (INS). A Kalman filter is implemented in the ECEF frame as a tracking filter with 12 states: position, velocity, velocity-bias, and acceleration state for each of the 3 axes. Velocity measurements from the INS and dGPS position measurements are used as observations. By comparing the INS velocity to the velocity obtained by numerically differentiating the dGPS position inputs, the velocity bias state is created. The acceleration state is driven by white noise. The final observation vector ($\Lambda_K$) has 9 elements; each of the 3 axes has a dGPS-derived position estimate, an INS-derived velocity, and an estimate of the bias between the INS-derived velocity and the dGPS derived velocity.[12]

$$\Lambda_K = (X_{GPS}, \dot{X}_{INS}, \delta\dot{X}_{GPS-INS}, Y_{GPS}, \dot{Y}_{INS}, \delta\dot{Y}_{GPS-INS}, Z_{GPS}, \dot{Z}_{INS}, \delta\dot{Z}_{GPS-INS})^T_{ECEF}$$

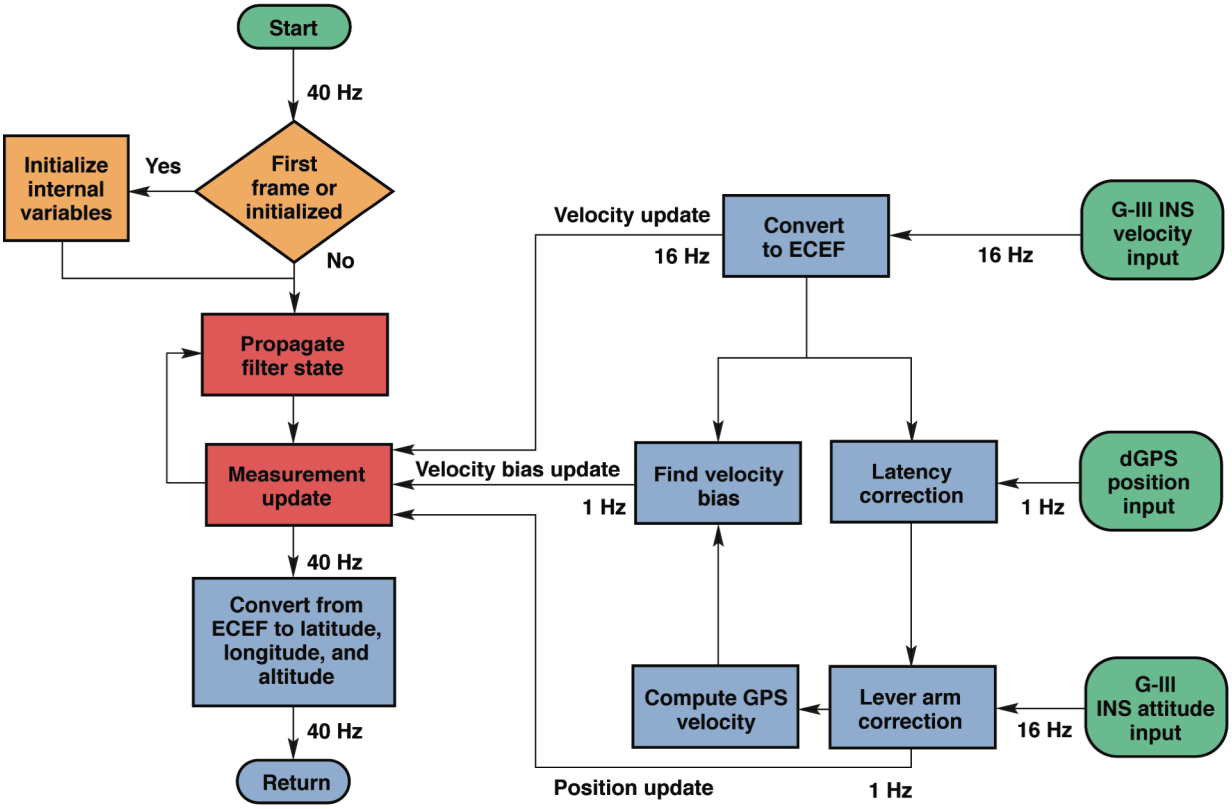


**Figure 5. Architecture of the navigation (Kalman filter) routine.**

The filter states were chosen to simplify construction of the state and observation update rules. The ECEF coordinates were chosen for the positions and velocities to allow the state update for the three axes to be decoupled. The state and observation vectors were chosen so that each observation directly corresponds to one of the states, simplifying the filter update. The corrected position is used directly as the true position measurement with no bias term built into the state vector. In the end, the position outputs are converted from the ECEF coordinate frame to latitude, longitude, and altitude for use by the guidance routine.

### C. Guidance Routine

The guidance routine consists of Simulink® block diagrams and embedded MATLAB® code. The main function in the guidance routine computes the intermediate waypoints that define the course line. The latitude and longitude for the start and end waypoints and the course type are required inputs for this routine. The course type can be selected as a constant heading (loxodromic) or great circle and shortest distance (geodetic), as shown in Fig. 6. Both course types are computed using the World Geodetic System 1984 (WGS 84) geodetic Earth model.[13] The loxodromic code is based on heritage FORTRAN code provided by JPL, and the great circle code uses an iterative Bessel solution.[14] Both course types were tested within a degree of latitude of the poles, 180-deg meridian crossings, and equatorial crossings in simulations. The guidance continuously outputs a set of intermediate waypoints along the desired ground track, which define an intermediate course segment.

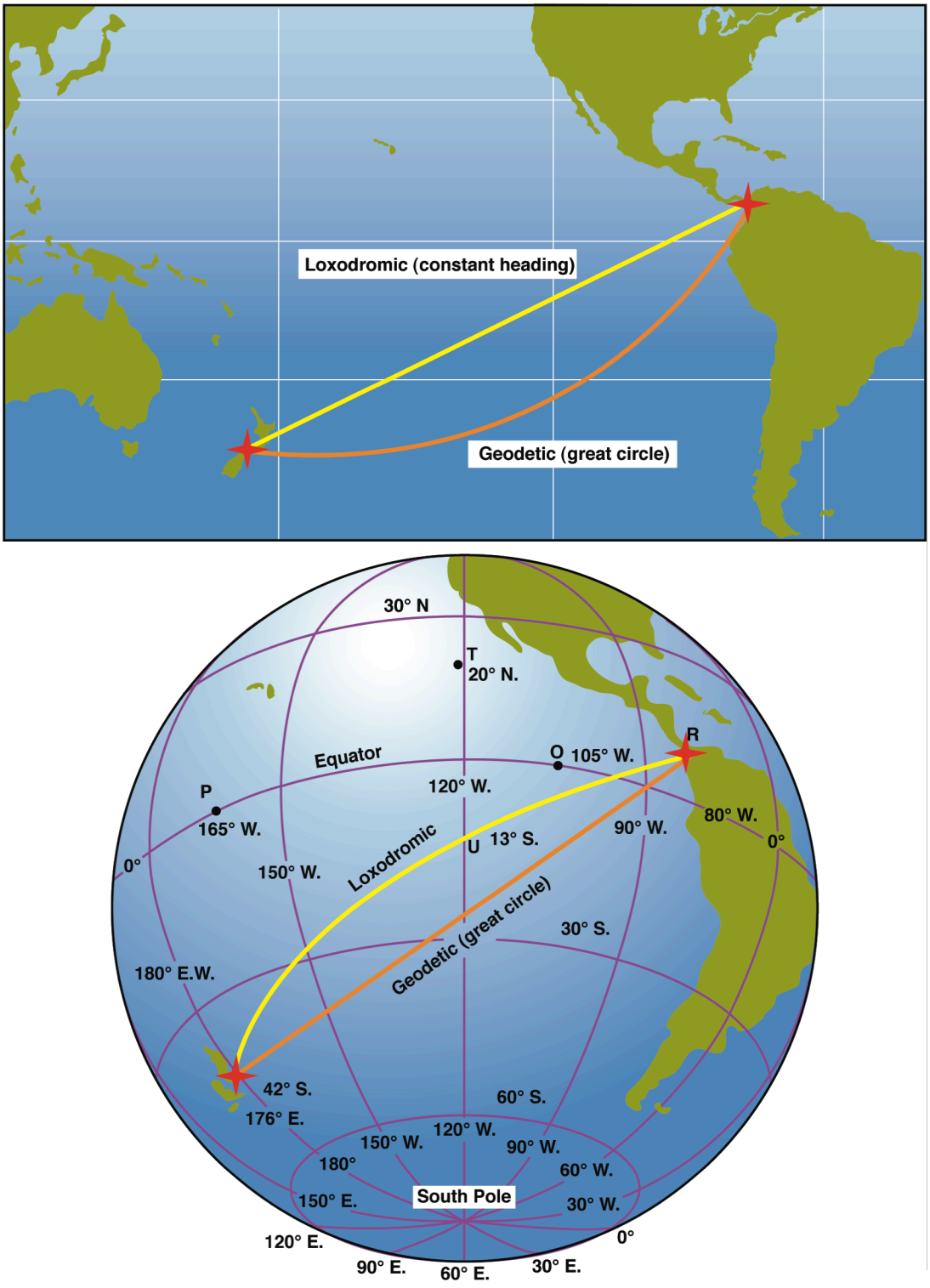


**Figure 6. Comparison of loxodromic (constant heading) and geodetic (great circle) trajectories.**

The intermediate course segment and current aircraft latitude and longitude from the navigation routine are used to compute a crosstrack error in feet. In lieu of using a crosstrack error derivative in the controller, a heading error is computed by subtracting the current intermediate segment true heading from the aircraft track heading (includes wind corrections).

The guidance routine also produces an altitude error by subtracting a defined reference altitude from the current aircraft altitude. The source of the aircraft altitude can be selected from either the navigation routine or from the pressure altitude, which is derived from the aircraft systems.

Once altitude and crosstrack errors are calculated, they are sent to the controller routine. In addition, another function of the guidance routine sets a Boolean flag true when the combined radial magnitude of the altitude and crosstrack errors is less than 5 m.

### D. Controller Routine

The PPA control consists of two proportional-integral-derivative controllers, one for the localizer axis and the other for the glide slope axis. Within the localizer controller (Fig. 7), the localizer proportional loop applies a gain to the crosstrack error and limits the output to reduce the maximum course intercept angle. The overshoot of the specified trajectory is kept small by limiting the course intercept angle. Additionally, to slow the initial turn to intercept the course, the proportional loop is faded in over a period of 2 s once the PPA is engaged. The localizer integral loop is driven by the crosstrack error signal. When the PPA is engaged, the integrator is reset to prevent a large initial offset. The localizer integral loop is active only when the magnitude of the crosstrack error is less than 300 ft for more than 30 s. This limitation reduces integrator windup and allows the proportional and derivative loops to stabilize near the course before the integral loop removes the remaining course offset. The integral output is constrained to half the aircraft flight director command limits to prevent saturation of the flight director's control loop. The localizer derivative loop is driven by the track heading error calculated in the guidance routine. To improve damping during course intercept, a lead filter is applied to the track heading error signal. Moreover, to accommodate larger initial course offsets, the derivative gain is reduced when the crosstrack error is greater than 1000 ft.

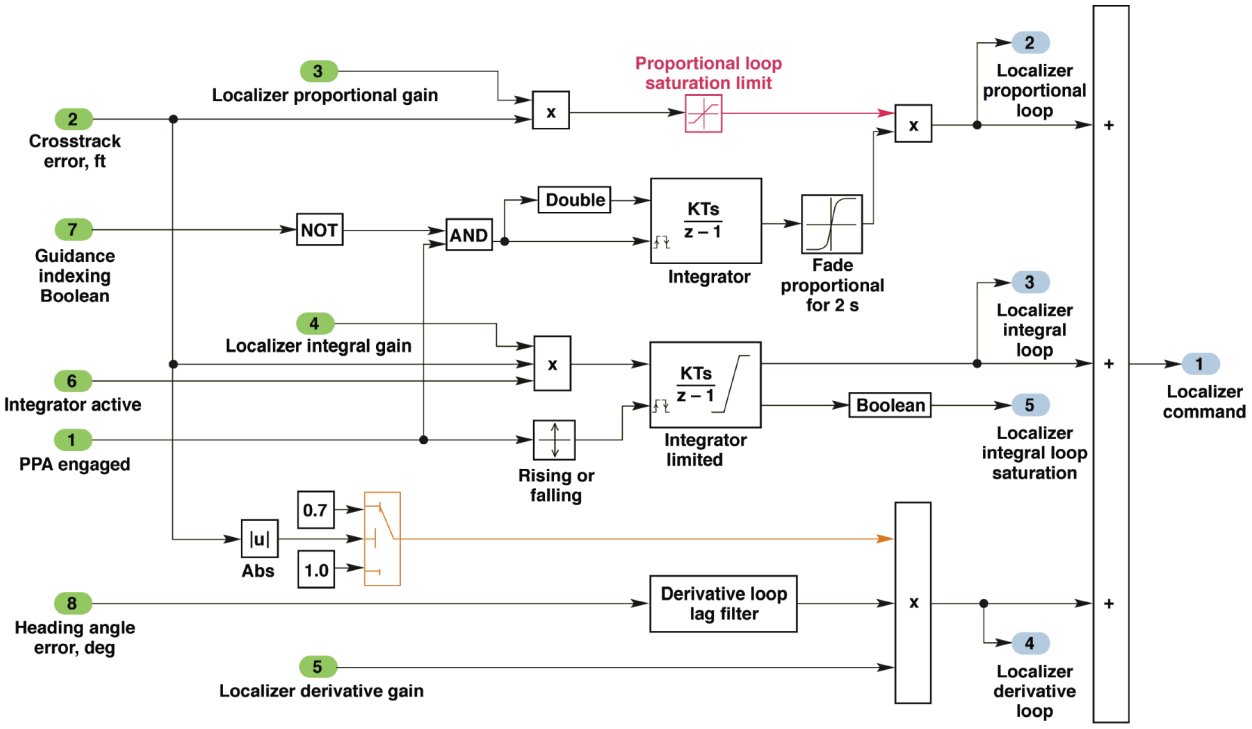


**Figure 7. Platform Precision Autopilot localizer path architecture.**

The glide slope controller, as illustrated in Fig. 8, is similar to the localizer channel and is driven by the altitude error, which has been passed through a lead filter. Similar to the localizer integral loop, the glide slope integral loop is reset when the PPA is engaged, active only when the altitude error is less than 150 ft for more than 15 s, and limited to half the flight director command limits. The glide slope derivative loop is driven by the aircraft inertial vertical velocity and is faded in over 5 s to reduce the load factor when the PPA is engaged. For increased damping, pitch rate feedback, which is provided by the aircraft systems, is also used. Outside the two controllers, scale factors

and biases are applied to the commands to counter the effects of the aircraft systems, which are described in section VI., A., "Instrument Landing System Interface System (I2S) and Navigation Receiver."

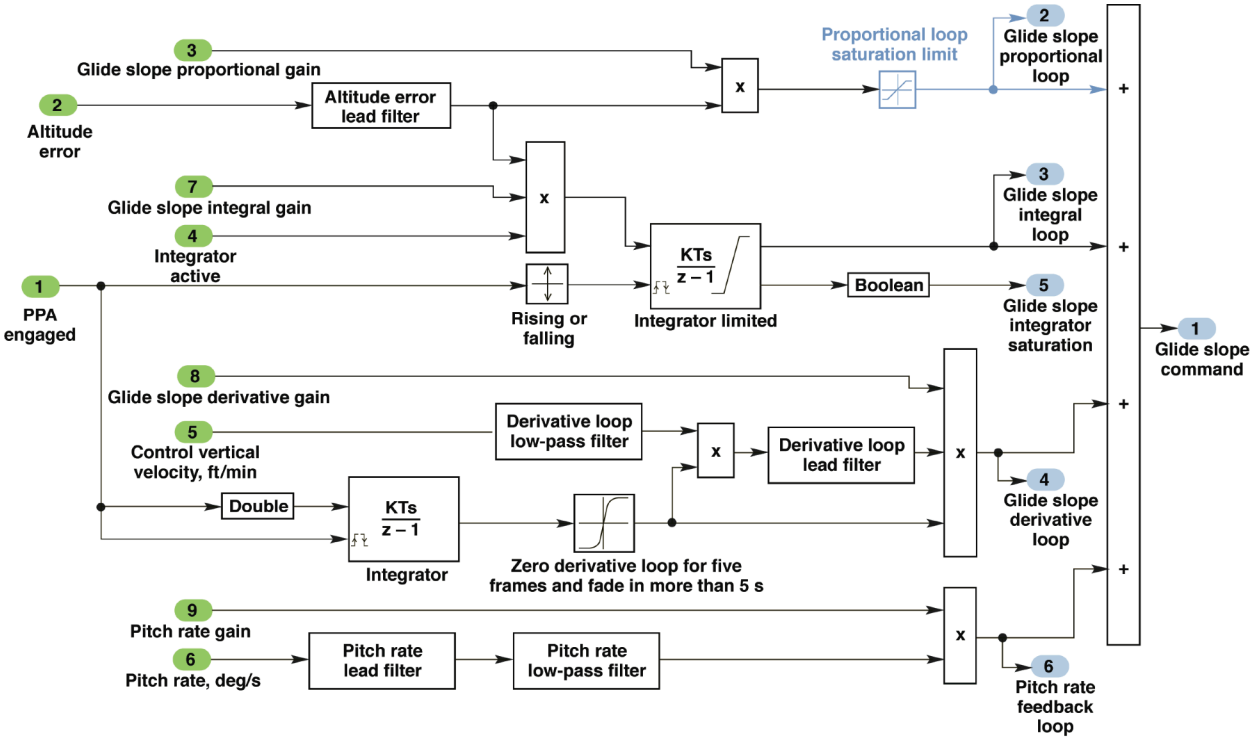


**Figure 8. Platform Precision Autopilot glide slope path architecture.**

## V. Platform Precision Autopilot Control Routine Development

The PPA controller was developed using several methods, including linear analysis, nonlinear simulation, Monte Carlo analysis, subsystem level testing, and hardware-in-the-loop (HIL) simulation. The design of the PPA controllers involved a process that started with linear analysis and then moved on to the nonlinear simulation. These two steps were iterated multiple times until adequate results were achieved, in which case the testing would proceed to Monte Carlo analysis with the nonlinear simulation, subsystem level testing, and HIL simulation. Additionally, ground and flight tests were used to verify aircraft system functionality and simulation models.

### A. Linear Analysis Tool

A linear model of the G-III was developed in MATLAB® and Simulink® for the PPA controller design. This simulation consisted of a linear aerodynamics model, PPA controller routine, G-III autopilot, G-III control surface actuator, and G-III sensor package models. Using a linear analysis tool developed at DFRC, a user could choose either the localizer or glide slope controller to perform gain design and analysis. The linear analysis tool had the capability to design gains using the root locus method of sequential loop closures to place the system poles at desired locations. Once each feedback loop gain was selected, all loops were closed to determine whether the 3-dB gain margin and 30-deg phase margin target was met. Time response performance (minimizing rise time, settling time, and maximum overshoot), with the aircraft initially offset by 100 ft in either crosstrack or altitude, also determined the acceptability of selected gains. This process was repeated for a number of flight conditions in the PPA envelope. For all design flight conditions, stability margins exceeded 6 dB in gain and 45° in phase.

### B. Nonlinear Simulation

A G-III nonlinear simulation was created to support additional PPA controller development. The basic architecture of the G-III simulation is the DFRC core simulation, which is a six-degree-of-freedom nonlinear simulation. This simulation consists of FORTRAN, C++, and Java™ code (Sun Microsystems, Inc., Santa Clara, California). The DFRC simulation includes equations of motion, an atmospheric model, discrete gust and turbulence models, an aerodynamic linearizer, numerical integration algorithms, and an analog-to-digital hardware interface.[15]

The G-III aircraft specific models come from a variety of sources. Code from a Federal Aviation Administration Level D pilot training simulator is the source of several aircraft models, including aircraft autopilot, avionics, aerodynamics, engine, and mass properties. The G-III simulation's Dutch roll, short period, and engine dynamics were validated against Gulfstream certification flight data. Models of the aircraft interface with the AIC, flight director, actuators, and sensors were developed in MATLAB® and Simulink® and converted to auto-code for integration into the simulation. The algorithm components of the PPA flight software were also auto-coded and integrated into the nonlinear simulation for analysis and verification and validation testing.

At the beginning of the controller gain design process, the nonlinear simulation was used to examine the time history performance of the controller with the nominal aircraft models. The simulation was then used to fine-tune the gains that were initially selected from linear analysis. Monte Carlo analysis was then used to examine robustness during nominal and off-nominal conditions in conjunction with the Monte Carlo analysis.

### C. Monte Carlo Analysis

The Monte Carlo analysis was implemented as an iterative brute force method to examine the robustness of the PPA to uncertainties. The procedure consisted of generating input scripts, running nonlinear simulations, and analyzing simulation output. Approximately 50 input parameters were randomly varied, including winds, aerodynamic coefficients, mass properties, initial conditions, and aircraft systems performance, to verify acceptable aircraft behavior and PPA performance. A set of metrics was developed to assess tracking performance from 150 s after PPA engagement to the end of the run for different gain sets and software versions. The following principle criteria were used to evaluate the tracking performance during the Monte Carlo analysis:

- $\sqrt{(altitude \quad error)^2 + (crosstrack \quad error)^2} < 5$ meters
- $\Delta$ normal acceleration < 0.1 $g$
- pitch rate < 0.5 deg/s and roll rate < 1 deg/s

### D. Subsystem Level Testing

During the PPA development, the software underwent several stages of verification and validation testing to flight-qualify the software, verify that the software requirements were met, and validate the system performance. Subsystem and software level tests involved the use of a series of automated MATLAB® scripts to verify the functionality of the PPA routines. Each script that was generated exercised all software logic and conducted specific tasks that verified each subsystem's adherence to performance requirements.

### E. Hardware-in-the-Loop

The HIL simulation environment (Fig. 9) was used extensively to test the AIC and validate the performance of the PPA hardware and software in closed-loop testing. The HIL simulation was run in real time and required several hardware interfaces for communication with the AIC. These interfaces consisted of an EtherNet® interface with the DCAPS simulator for bidirectional UDP packets, a serial interface (RS-422) for differential GPS inputs, and a shared-memory interface. The tests conducted on the HIL simulation centered on two objectives: validating that the AIC meets flight hardware requirements, and validating that the PPA control algorithms perform as designed in nominal and off-nominal flight conditions and with simulated hardware and software failures. In the end, the HIL simulation was the main determinant of whether to proceed to on-aircraft ground testing and flight-testing.

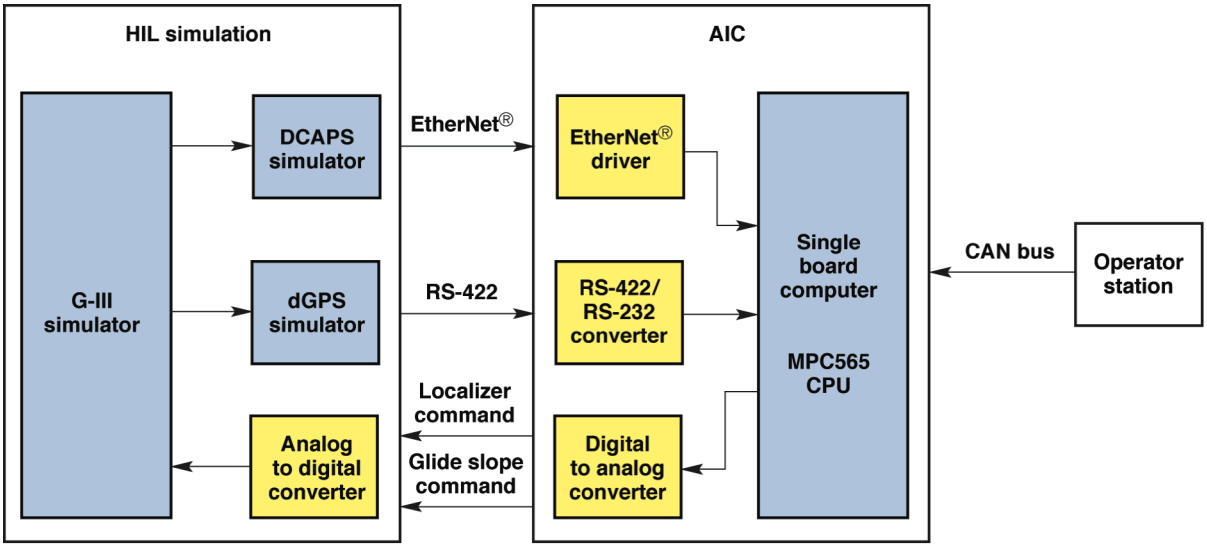


**Figure 9. Platform Precision Autopilot hardware-in-the-loop simulation architecture.**

## VI. Subsystem Testing

Three subsystems that required special attention were the I2S, navigation receiver, and flight director. Because of the unavailability of complete documentation, these systems required extensive testing to characterize their performance. The initial tests were conducted on the ground for all three systems to develop preliminary simulation models.

### A. Instrument Landing System Interface System (I2S) and Navigation Receiver

The I2S and aircraft navigation receiver make up the path for the PPA commands from the AIC to the aircraft flight control system. Through ground testing, it was discovered that this combination amplifies the PPA output by 20 percent and adds a bias to the receiver output. Hence, a nonzero command from the PPA is required to achieve a 0-mV receiver output corresponding to no change in command to the G-III autopilot. Moreover, output from the navigation receiver is amplified through the flight director before reaching the G-III autopilot. Both the glide slope and localizer channels exhibited low-frequency drift. For these reasons, zeroing the navigation receiver output is essential for the PPA to function appropriately.

While the PPA is engaged, the controller integral loops have plenty of authority and are quick enough to remove any given combination of the effects discussed in the previous paragraph. Any nonzero navigation receiver output that is present at the PPA engagement, however, will cause an initial vertical velocity and roll transient that increases the time required to intercept the course in both altitude and crosstrack. As a result, an algorithm was created and implemented into the operator station software. This algorithm allows the operator to add a bias to the PPA commands to zero the navigation receiver output whenever the magnitude is greater than approximately 15 mV before starting a new track.

### B. Flight Director

During the PPA development, detailed knowledge of the flight director's operation was lacking; the available documentation was not detailed enough to attain complete insight into the flight director's operation. As a result, there were concerns about the operation of the ILS approach mode at cruise speeds. These concerns resulted in ground testing of the flight director in an attempt to characterize its operation. These tests were inconclusive and did not provide definitive data on the flight director's operation. In addition, determining the flight director response to INS inputs was difficult using a stationary aircraft. Bench testing of the flight director was planned to accurately characterize the flight director; however, it was later abandoned in favor of flight-testing. The PPA controller was modified for additional robustness to account for the uncertainties in the flight director operation.

## VII. Flight-Testing

The PPA flight test was divided into cycle 1 and cycle 2 flight activities, both conducted without the SAR pod attached to the G-III. Early pod clearance flights established that the radar pod does not significantly affect aircraft dynamics. The flight test program began in March 2007 and lasted for 8 months, with 7 flights conducted in cycle 1 and 13 flights conducted in cycle 2. This section provides an overview of the cycle 1 and cycle 2 flight sets. The next section, "Flight Test Results," presents the details of the PPA performance during the flight tests.

The primary objective of the cycle 1 flights was to evaluate the models of the G-III and associated systems including the navigation receiver, flight director, and factory G-III autopilot. A secondary goal for the cycle 1 flights was to demonstrate meeting the 5-m radius tube for two representative flight conditions.

The first three cycle 1 flights were performed with an open-loop controller, in which the PPA issued step commands to the aircraft systems without operation of the feedback controller. During the first cycle 1 flight, it was discovered that the flight director performed a pitch down maneuver at PPA engagement for 15 s with a nearly centered glide slope needle (zero PPA command). This preprogrammed flight director behavior was designed to ensure that the aircraft descends to capture the glide slope for an actual ILS approach with less overshoot. This initial pitch down is obviously undesirable for a constant altitude UAVSAR mission. After further research of the flight director documentation, a solution was found to deal with the pitch down command. The autopilot servos could be disabled during the pitch down maneuver by depressing the touch control steering (TCS) button located on the control yoke. During the second flight, the copilot depressed the TCS button prior to PPA engagement and manually stabilized the flight path until the flight director pitch cue returned to a neutral position. The TCS was then released, allowing the PPA to be coupled to the G-III autopilot. This procedure became the standard for all successive flights.

After the first cycle 1, closed-loop controller flight (at a mean sea level of 35,000 ft and a Mach number of 0.75), the PPA localizer and glide slope gains were refined, and the flight director pitch angle and pitch rate limits were better modeled from the flight data. This data revealed that the flight director gains were three times higher than previously measured from ground testing. The flight director, which receives input from the radar altimeter, adjusts its gains when the aircraft is more than 1200 ft above ground level. This gain adjustment accounted for some of the gain disparities between the ground and flight tests. Many attempts were made during the initial flights to determine gains for other flight director inputs, including vertical velocity and roll angle, using flight data analysis; however, these attempts did not result in definitive answers. Instead, as discussed previously, the PPA was made more robust to compensate for the uncertainties in modeling the flight director performance.

The second cycle 1 flight condition (at a mean sea level of 30,000 ft and a Mach number of 0.8) was lower and faster. The PPA gains for this condition were very similar to the 35,000-ft, Mach-0.75 flight condition. As soon as acceptable PPA performance was obtained at both flight conditions along north-south and south-north trajectories, the PPA was then tested with different heading trajectories to test the guidance routine.

Once the PPA was sufficiently tuned with cycle 1 data, cycle 2 flights were designed to map out the flight envelope shown in Fig. 10, determine the flight conditions in which the requirements are met, and conduct further adjustments to the PPA routines. The candidate flight envelope was selected from the cruise section in the G-III flight manual performance data. Altitudes ranged from 25,000 ft up to the service ceiling at 45,000 ft. The speed regime extended from the maximum specific range (MSR) at empty weight to the G-III maximum speed limit (Mach 0.85 or 340 KIAS). Furthermore, a low-speed "cushion" of approximately Mach 0.05 was added at each altitude tested.

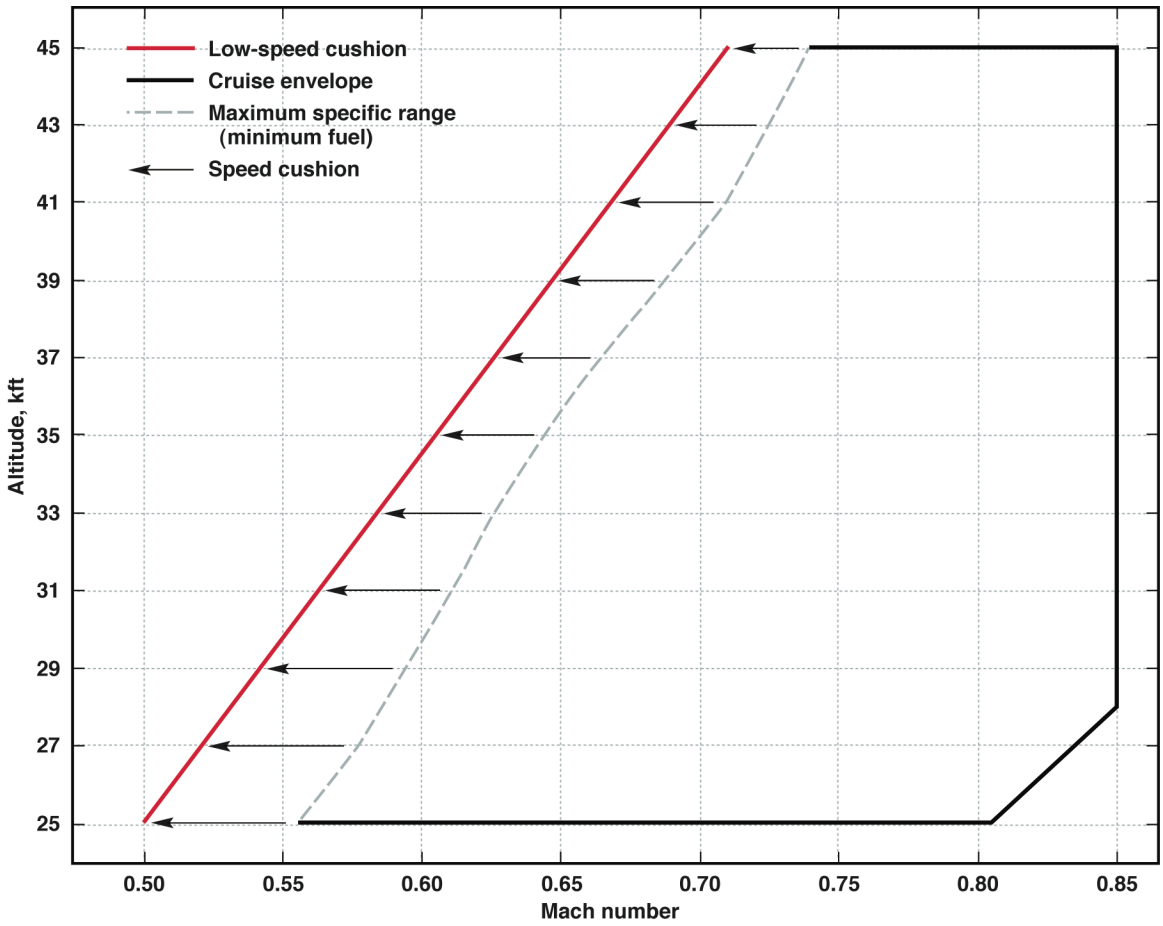


**Figure 10. Flight envelope for which the Platform Precision Autopilot was tested; low-speed cushion of approximately Mach 0.05 was incorporated.**

During the cycle 2 envelope expansion at comparatively slower true airspeeds, the flight director pitch rate limit was found to increase as airspeed decreased. At faster airspeeds, the PPA command was exceeding this rate limit most of the time. The comparatively higher pitch rates degraded the altitude tracking performance and produced a heaving motion of ± 0.1 *g* normal acceleration for a period of approximately 5 s. To resolve this issue, the Monte Carlo tool, with increased uncertainties in the flight director model, was used to evaluate modifications to the PPA controller. In turn, the PPA controller was given pitch rate feedback, which succeeded in lowering the commanded pitch rates.

## VIII. Flight Test Results

This section describes the PPA performance during the flight tests. Results from the cycle 1 and 2 flight tests, and postflight tests are presented.

### A. Cycle 1 Flight Test Results

For both flight conditions tested during the cycle 1 flights, the 5-m radius tube requirement was met. Figure 11 is a contour plot of the percentage of time the reference point on the G-III was inside the 5-m radius tube for a flight run at an altitude of 35,000 ft and a Mach number of 0.75. For 90 percent of the time, the PPA controlled the G-III within ± 3 m of crosstrack and -1 to +3 m of altitude.

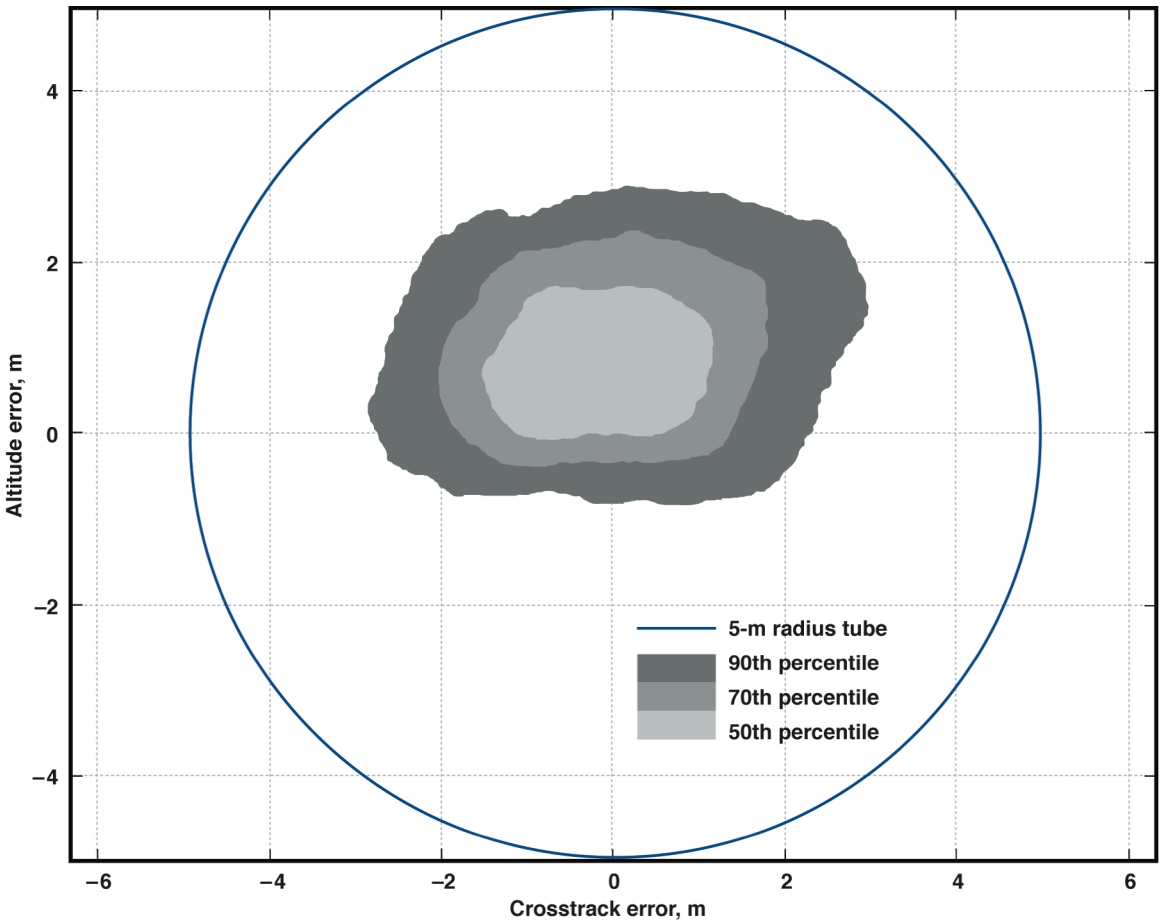


**Figure 11. Percentile contour plot of a cycle 1 flight segment; flight 5, 35,000 ft, Mach 0.75.**

An additional desired goal was to simultaneously minimize the Euler angles and Euler rates while remaining in the 5-m radius tube. The Euler angles (Fig. 12), during the same segment shown in the previous figure, did not exceed JPL's desired maximum value of a 5-deg peak-to-peak variation for the pitch and roll angles and a 15-deg peak-to-peak variation for the yaw angle. During this specific flight, less than 4-deg roll angle, 1-deg pitch angle, and 0.5-deg yaw angle peak-to-peak variations were observed. The angular rates were within approximately ±1 deg/s roll rate, ±0.5 deg/s pitch rate, and ±0.25 deg/s yaw rate (Fig. 13). These desired angles and rates were met more than 90 percent of the time on this flight segment.

The second flight condition at an altitude of 30,000 ft and a Mach number of 0.8 demonstrated similar performance (Fig. 14). At this comparatively faster true airspeed, the flight director pitch rate limit was 12 percent lower, making any pitch oscillations even smaller.

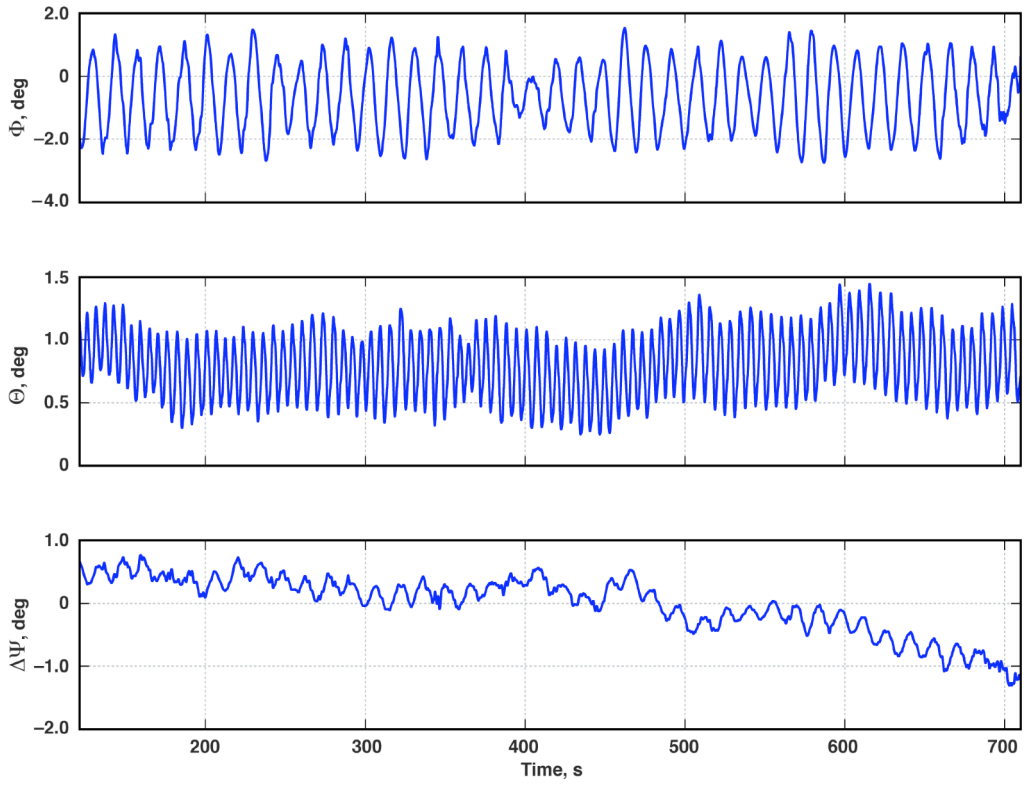


**Figure 12. Euler angles experienced during a cycle 1 flight segment; flight 5, 35,000 ft, Mach 0.75.**

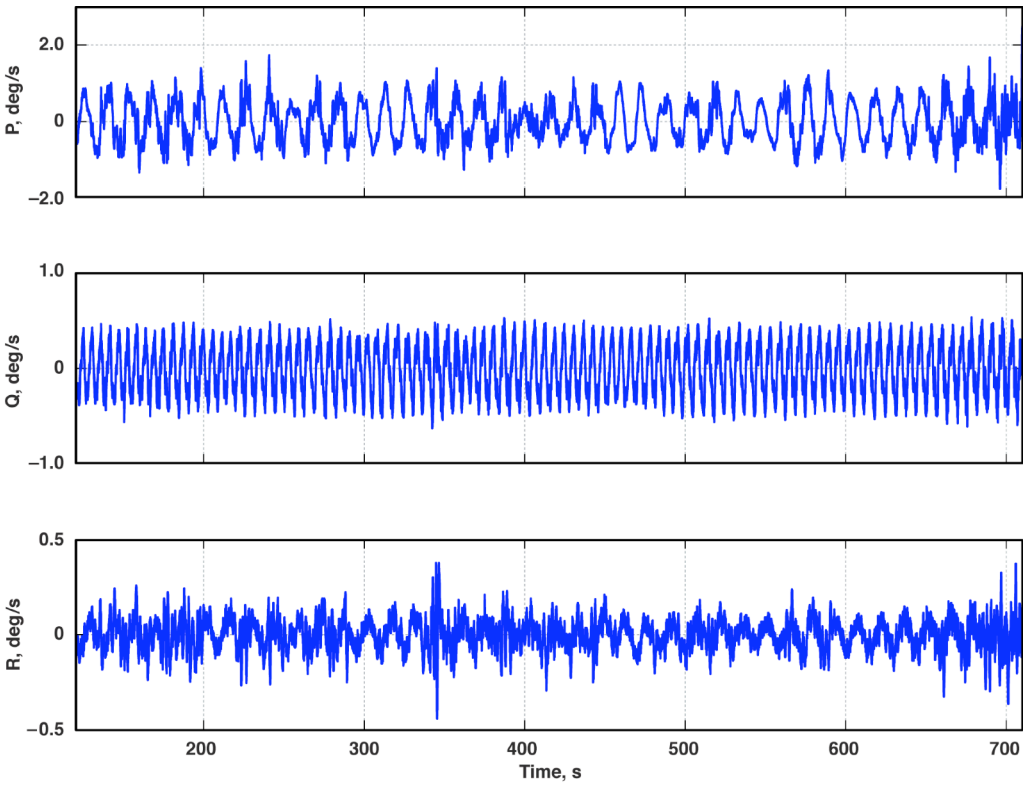


**Figure 13. Euler rates experienced during a cycle 1 flight segment; flight 5, 35,000 ft, Mach 0.75.**

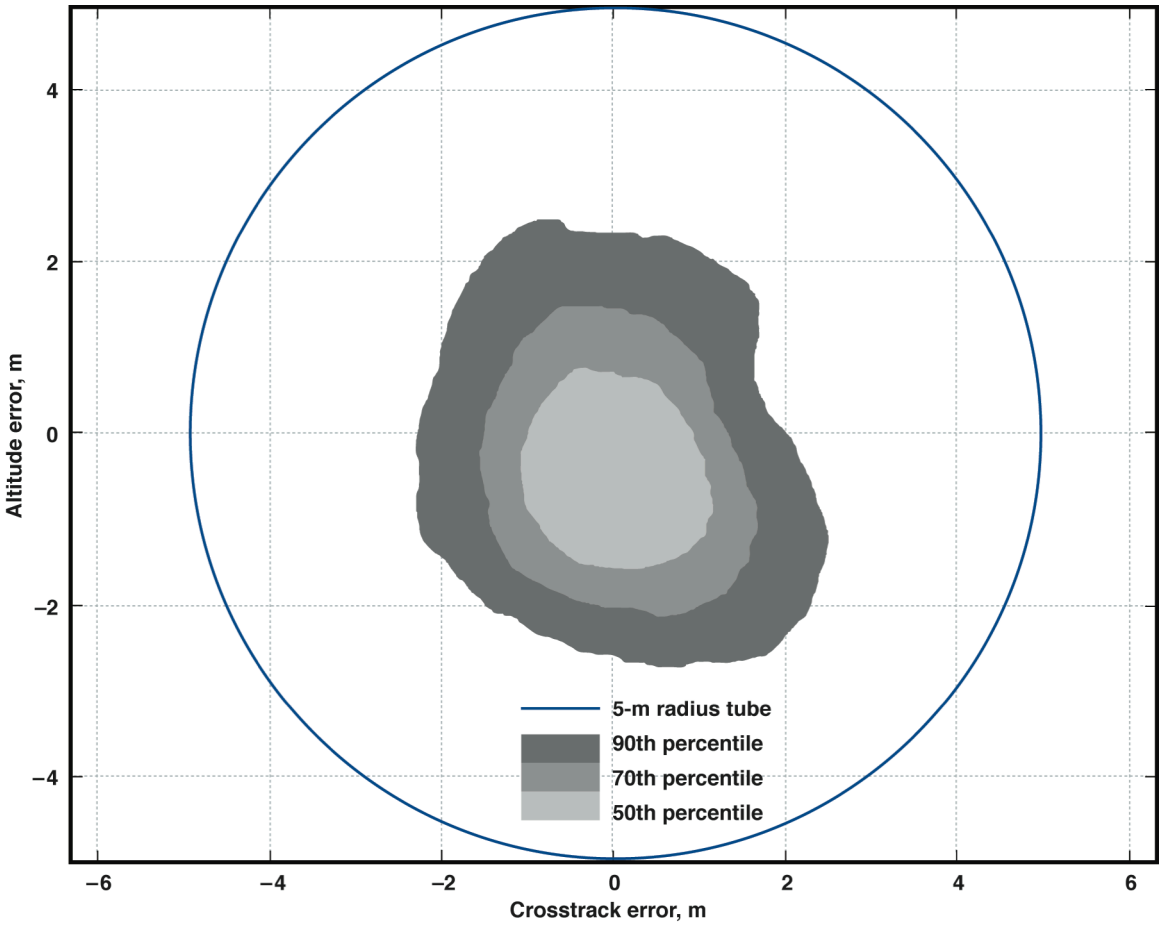


**Figure 14. Percentile contour plot of a cycle 1 flight segment; flight 5, 30,000 ft, Mach 0.80.**

### B. Cycle 2 Flight Test Results

Figure 15 shows results for the cycle 2 evaluation flights. The circles at each flight condition represent the 5-m radius tube. The outer margin of the embedded contour plot encompasses 90 percent of the flight track time for that flight condition. Generally, there was adequate performance to keep the G-III inside (or within a meter) of the tube boundary more than 90 percent of the time for each flight segment.

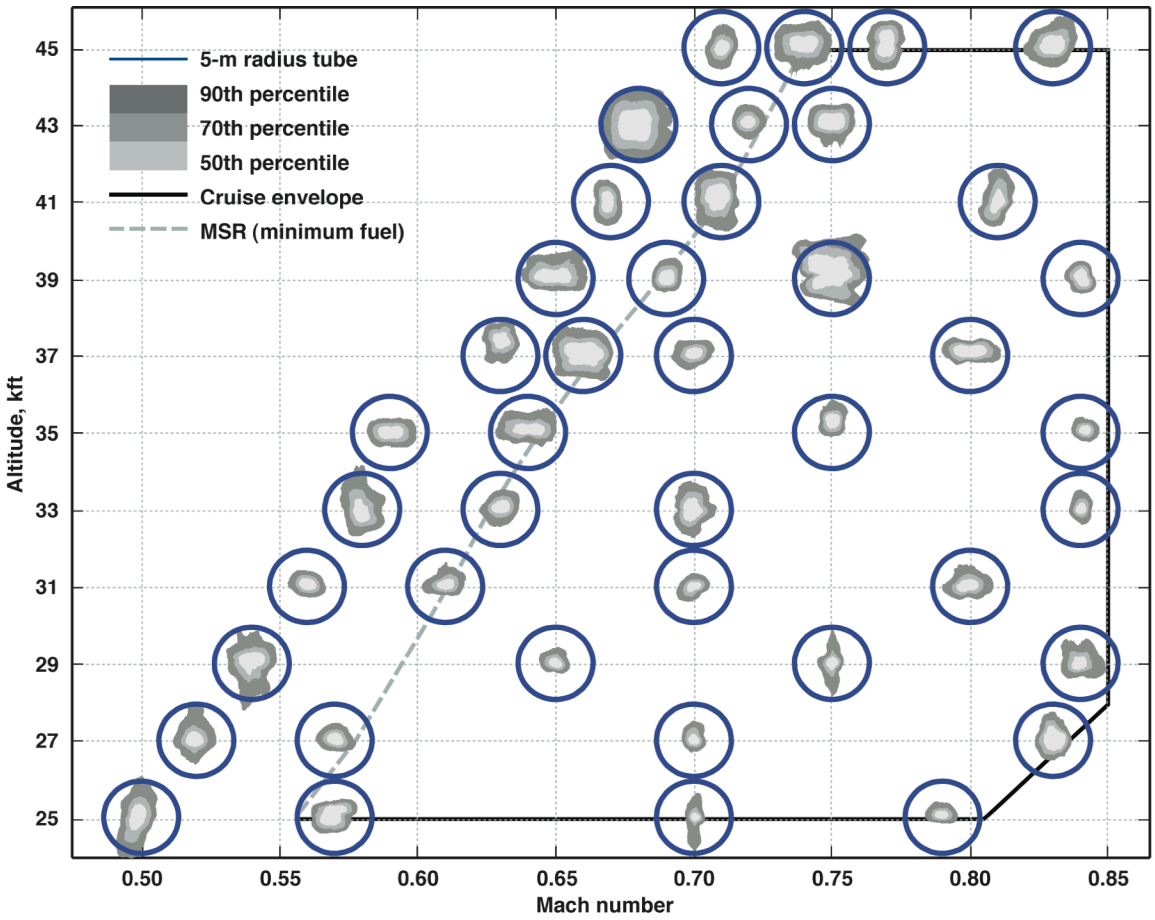


**Figure 15. Cycle 2 flight envelope with outer contours encompassing 90 percent of flight time at each flight condition.**

During a SAR data collection, maintaining a nearly constant ground speed is important to obtaining the highest quality SAR images. Without an auto-throttle capability on the G-III, the pilots have to manipulate the throttles to maintain a nearly constant ground speed while flying through air with varying winds on a given track segment. When the pilots increased the throttle to maintain ground speed, the aircraft would climb, and would conversely descend when the throttle was reduced. The PPA controller eventually took out the altitude error, typically over a period of 15 to 30 s.

The Euler angles (pitch, roll, and yaw) were all within the desired range during each flight segment for more than 90 percent of the time at each flight condition. Figure 16 shows 90$^{th}$-percentile angular rates for representative altitude ranges, low (25,000 to 31,000 ft), middle (33,000 to 39,000 ft), and high (41,000 to 45,000 ft), as a function of Mach number. The pitch and yaw rates were well within the desired 0.45 deg/s for all flight conditions for more than 90 percent of the time. The roll rate was within 1.5 deg/s for each flight condition more than 90 percent of the time. As a general rule, all angular rates were lower at the comparatively higher dynamic pressure flight conditions.

Because of the number of flight conditions tested, cycle 2 flights were conducted on a number of days with considerable variation in atmospheric stability, lifting action, turbulence, and temperature. The flights were generally on the eastern (leeward) side of the Sierra Nevada Mountain range in a north-south direction, a region known for frequently unstable air. The variation in G-III performance under PPA control can, in part, be attributed to these factors.

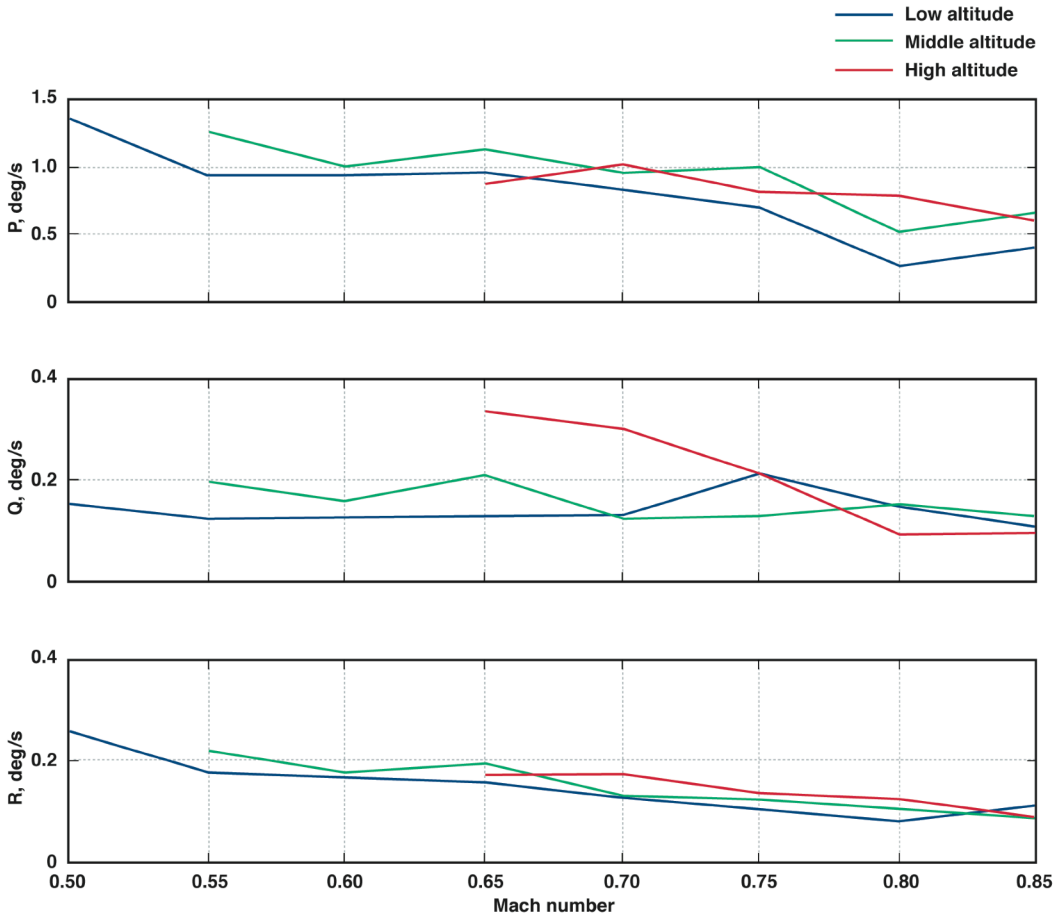


**Figure 16. The 90th-percentile Euler rates as a function of Mach number for representative altitude ranges during cycle 2 flights; low altitude (25,000 to 31,000 ft), middle altitude (33,000 to 39,000 ft), and high altitude (41,000 to 45,000 ft).**

### C. Postflight Test Science Results

Since the end of PPA flight tests, the UAVSAR program has conducted several science missions over Mount St. Helens, the Salton Sea, and California fault lines using the PPA. For most of these flights, the PPA has exceeded the 5-m radius tube requirement. For 80 SAR data runs spread over 12 flights, the PPA has controlled the G-III within ± 2.5 m in altitude and crosstrack more than 90 percent of the time (Fig. 17).

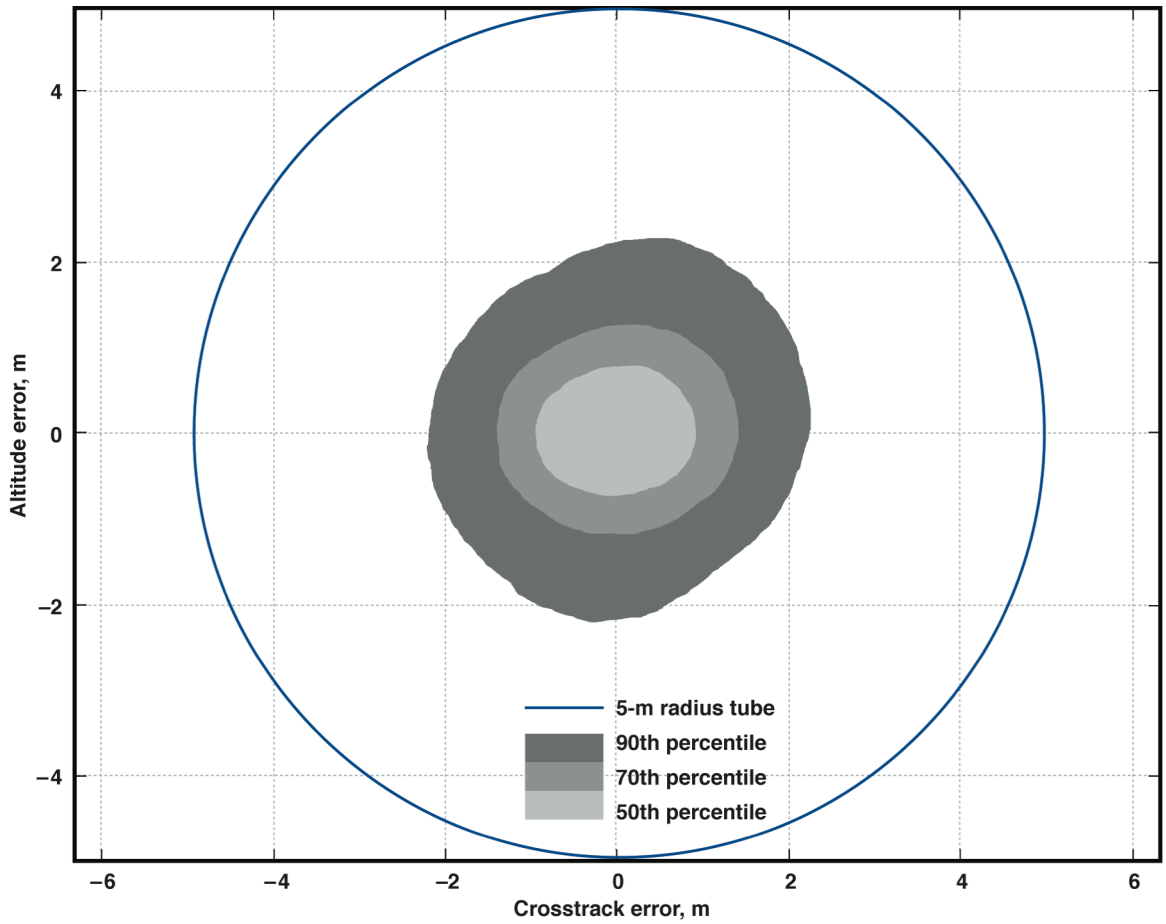


**Figure 17. Postflight testing: Platform Precision Autopilot exceeding the 5-m radius tube objective for all of JPL's science mission flights; 80 data runs spread over 12 flights; total flight time, 11 hours.**

## IX. Conclusion

A Platform Precision Autopilot (PPA) has been developed and flight tested to support the NASA Uninhabited Aerial Vehicle Synthetic Aperture Radar (UAVSAR) program. Through flight-testing, the PPA has demonstrated that it meets the requirement of flying within a 5-m (16.4-ft) radius tube for distances to 200-km (108-nmi) long in the presence of light turbulence for 90 percent of the time. This capability allows precise, repeat-pass interferometry for the UAVSAR program, whose primary objective is to develop a miniaturized, polarimetric, L-band synthetic aperture radar for repeat-pass interferometry. The PPA interface method minimizes system modifications to the baseline Gulfstream III jet and retains the inherent system safety features of the flight director and Gulfstream III jet autopilot. The PPA has demonstrated the ability to control an aerial platform very precisely while minimizing unwanted motion, and it did so with minimal impact to the integrity, certification, and inherent safety features of that platform. The PPA system has been successfully used in the field for science missions since December 2007. The customer, Jet Propulsion Laboratory, has noted that the PPA performance most often exceeds the requirements.

## References


[1]Donnellan, A., Fielding, E., Glasscoe, M., Holt, B., Kwok, R., et al., "InSAR Workshop Summary Report," *InSAR Workshop*, JPL 400-1240, NASA, 2004.

[2] Zebker, H.A., Farr, T.G., Salazar, R.P., and Dixon, T.H., "Mapping the World's Topography Using Radar Interferometry: the TOPSAT Mission," *Proceedings of the IEEE*, Vol. 82, No. 12, IEEE, New York, 1994, pp. 1774–1786.

[3] Rosen, P.A., Hensley, S., Joughin, I.R., Li, F.K., Madsen, S.N., Rodriguez, E., Goldstein, R.M., "Synthetic Aperture Radar Interferometry," *Proceedings of the IEEE*, Vol. 88, No. 3, IEEE, New York, 2000, pp. 333–382.

[4] Van Zyl, J.J., "Overview of SAR Polarimetry and Interferometry," *Proceedings of the SPIE*, Vol. 3120, JPL TRS 1992+ 97-1538, 1997, pp. 16–27.

[5] Wheeler, K., Hensley, S., Lou, Y., Miller, T., and Hoffman, J., "An L-Band SAR for Repeat Pass Deformation Measurements on a UAV Platform," *2nd AIAA "Unmanned Unlimited" Systems, Technologies, and Operations*, AIAA 2003-6619, 2003.

[6] Lou, Y., Kim, Y., and van Zyl, J., "The NASA Airborne Synthetic Aperture Radar System," *Conference at the Jet Propulsion Laboratory*, JPL TRS 1992+ 96-0290, 1996.

[7] Lou, Y., Imel, D.A., Chu, A., Miller, T.W., Moller, D., and Skotnicki, W., "Progress Report on the NASA/JPL Airborne Synthetic Aperture Radar System," *2001 IEEE International Geoscience and Remote Sensing Symposium*, Vol. 5, IEEE, New York, 2001, pp. 2046-2048.

[8] Hensley, S., Wheeler, K., Sadowy, G., Jones, C., Shaffer, S., Zebker, H., et al, "The UAVSAR Instrument: Description and Test Plans," *2007 NASA Science and Technology Conference*, NASA, 2007.

[9] Madsen, S.N., Skou, N., Granholm, J., Woelders, K.W., and Christensen, E.L., "A System for Airborne SAR Interferometry," *AEU,International Journal of Electronics and Communications*, Vol. 50, No. 2, 1996, pp. 106-111.

[10] U.S. Department of Defense, "Flying Qualities of Piloted Aircraft," MIL-STD-1797A, Appendix A, 1990. (Contact: ASD/ENES, Wright-Patterson AFB, OH 45433-6503.)

[11] Hang, R., "Data Collection And Processing System (DCAPS): System Design Objectives Documents," NASA G3-DCAP-SDO-001, 2007.

[12] Grewal, M., Andrews, A.., *Kalman Filtering: Theory and Practice Using MATLAB®, 2nd Edition*, John Wiley & Sons, Inc., New York, 2001, Chapter 4.

[13] National Imagery and Mapping Agency, "Department of Defense World Geodetic System 1984," NIMA TR8350.2, 3rd Ed., Amendment 1, 2000.

[14] Borre, K., *Linear Algebra, Geodesy, and GPS*, Wellesley-Cambridge Press, Wellesley, MA, 1997.

[15] Norlin, K., "Flight Simulation Software at NASA Dryden Flight Research Center," NASA TM-104315, 1995.